Observation of 0.3 kHz to 500 MHz Periodic Oscillations in the PFRC-2 Device

E. Ho,* C. Swanson,† S. A. Cohen,† J. Liu,* J. Matteucci,† P. Jandovitz,† J. Pearcy,* and R. Oliver‡

(Dated: September 2015)

With a capacitively coupled 27-MHz RF system supplying up to 400 W of power at the end of the main chamber (MC), hydrogen plasma was generated in the Princeton Field-Reversed Configuration Device (PFRC-2), operating in a tandem mirror mode. Langmuir probes were used to measure oscillations in the floating potential in the satellite region (SR), at the other end of the PFRC-2. Oscillations indicate instabilities in the plasma. A fast camera was used to examine visible plasma oscillations in expansion region (ER). At speeds between 5 and 13 kiloframes per second (kfps), the fast camera showed oscillations below 700 Hz; corresponding peaks were found in the floating potential spectrum. Radial probe measurements suggest it to be a bursting m=0 mode. The probe data also measures the drive RF, at 27 MHz and its first 10 harmonics. A broad peak is near 300 MHz, close to the ER electron cyclotron frequency. Frequencies near 1 MHz, in the ion cyclotron resonance frequency of the mirror-coil field, varied linearly with the magnetic field strength. These intermodulate with the RF signal, creating sidebands to the 27 MHz peak and its harmonics. Using a probe with higher impedance, it was found that the floating potential measured around -250 V, indicating a population of electrons of a much higher temperature than originally expected. X-ray data collection in a related project supported this hypothesis.

I. INTRODUCTION

The difficulties in achieving controlled nuclear fusion are manifold, but the FRC offers a potential solution to several. Many plasma experiments are large and costly, while this may yield a small-scale alternative to fusion with confinement that requires a magnetic field of smaller magnitude. The PFRC-2 initially generates a plasma with a capacitively coupled 27-MHz RF system. This produces a column of plasma. Creating an FRC requires a rotating magnetic field (RMF), generated by coils located between the magnetic flux conserving rings, to form the separatrix, a region in the center of the plasma with closed magnetic field lines. Closed field lines allow for confinement, a key component of achieving fusion energy. Additional benefits of this configuration include the machine's small size and the high β value, which is the ratio of plasma pressure to magnetic field pressure. This makes the FRC more financially efficient, as higher magnetic field pressure requires more expensive equipment. Because it does not rely on a constantly changing electric current to drive the plasma, the FRC can operate in steady state, which is important for a reactor ultimately intended for fusion.

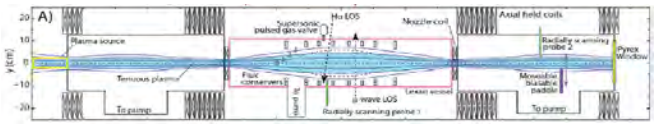

FIG. 1. Diagram of the PFRC-2 device.

Oscillations are found everywhere in the natural world, from the regularity of the Earth's orbit to the alternating current power in electrical outlets. In plasma, oscillations occur as a result of perturbations, to restore neutrality. Understanding the behavior of the oscillations of ions and electrons and interactions between those oscillations is key to analyzing how instabilities will grow and behave. The majority of the data in this paper were collected when the PFRC was in the tandem mirror mode, not an FRC, with a radially inserted Langmuir probe measuring the floating potential.

II. METHODS

Fig. 1 indicates the probe's location along the axis of the device, approximately 80 cm from the center of where the separatrix is located when running the RMF. The machine typically contains hydrogen gas, although some data was collected with argon inside. Gas flows into the machine from valves located at the end of the main chamber, and two pumps, located in the expansion region and the satellite region, maintain pressures in the range of 10-5 torr in the SR, which is between the nozzle coils and pyrex window on the right side in Fig. 1. The location of the 'gas valves and pumps maintain a higher pressure near the MC, between the plasma source and nozzle coils on the left in Fig. 1, than in the SR, where the probe is located. In the MC and ER, between the nozzle coils, pressures were in the range of 10-3 torr. Pressure was measured using a Residual Gas Analyzer (RGA) and an ion gauge in the SR. For all instances of data collection except one, the probe was connected to a 400 MHz oscilloscope. In the other situation, an oscilloscope with higher impedance was used to analyze the floating potential.

Several factors were varied without the RMF. The two pumps can be adjusted to increase or decrease pressure and density in the device, with the effects more pronounced in the SR because of its proximity to the pumps and distance from the gas valves. The power input of the RF source ranged from 75 to 300 W. Lower power would not sustain the plasma, while higher power heats the plasma, causing the potential of the probe to become too negative and risk damaging the oscilloscope. In some cases, power was modulated at 5 kHz rather than being held constant. The radial position of the probe itself could be changed, ranging from .25 to 4.6 cm from the

* Princeton University
† Princeton Plasma Physics Lab
‡ Brown University

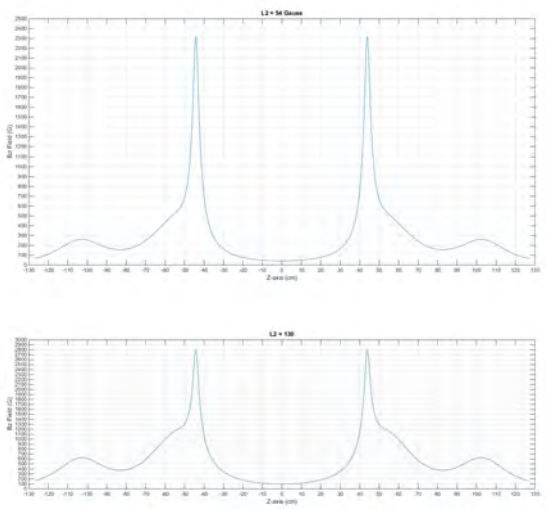

FIG. 2. Magnetic field along the z-axis at different L coil currents.

center. Additionally, the current through the main magnetic field coils (nozzle coils) and mirror magnetic field coils (L-coils), and therefore the magnitude of the applied magnetic field, were altered to create a B field scan profile. For nozzle coils at 300 A and L-coils at 54 and 130 A, the minimum and maximum values in our trials, Figs. 2(a) and 2(b) show the magnitude of the magnetic field along the axis of the device. The ranges are 50-2310 G and 100-2800 G respectively.

With the RMF generating an FRC, fewer adjustments were made. The probe was kept 0.25 cm from the center throughout all RMF data collection. RF power stayed in the same range as in the plasma column setup, between 75 and 300 W, while RMF power ranged from 8 to 20 kW. The RMF operated in pulses that lasted between 2 and 9 ms. A micropuff of hydrogen gas was introduced, timed to trigger at a certain time in each RMF pulse. The timing of this puff could also be changed to examine how instabilities grow before and after the release.

In these conditions, a fast camera recorded the field between the nozzle coils and flux conservers on the end closer to the SR. With frame speeds up to 121,212 fps, the plasma's oscillations could be observed. The camera's aperture was open as much as possible, while exposure time was adjusted as the camera was pointed at brighter or dimmer parts of the plasma. Phantom videos from the plasma column with argon and hydrogen were used to observe the frequency and spatial distributions of low frequency modes. The videos were also used to calculate a rough estimate of the time the plasma took to reach full brightness and to dim again after the RMF stopped within each pulse.

III. RESULTS

Name	Frequency Range	Method of Detection	Possible Causes
Lowest	527 and 676 Hz	Fast camera	M = 1 rotational mode
Bursting	400 Hz	Langmuir Probe	Turbo pumps
Low-range	1-2 MHz; often multiple peaks	Langmuir Probe	Ion cyclotron Ion plasma Electrostatic ion cyclotron Drift waves
Input	27 MHz; up to 8 harmonics	Langmuir Probe	RF signal
Intermodulating	25-29 MHz; sidebands around input signal	Langmuir Probe	Lower hybrid oscillation (interaction between RF signal and low-range)
Asymmetric intermodulating	25-29 MHz	Langmuir Probe	Parametric instability
High-range	300 MHz	Langmuir Probe	Electron cyclotron

While the magnetic field in the device was changed by altering the current flowing through the L-coils, we tracked the movement of the largest peak in the range of 1-2 MHz through this scan on several occasions. While the other conditions varied slightly between each separate run, the peak location as it related to the magnitude of the L-coil current remained consistent, following a linear trend.

One caveat, however, is that as the current dropped below 80A, the frequency structure became more complicated (Fig. 3), and it became uncertain whether or not we were following the same peak as more appeared. For instance, in Fig. 4(a), where the L-coil current is 115 A, it is clear which peak is the major one. However, when the current is 62 A, shown in Fig. 4(b), the more complex structure makes it difficult to determine if we are examining the same peak or if a new one arose.

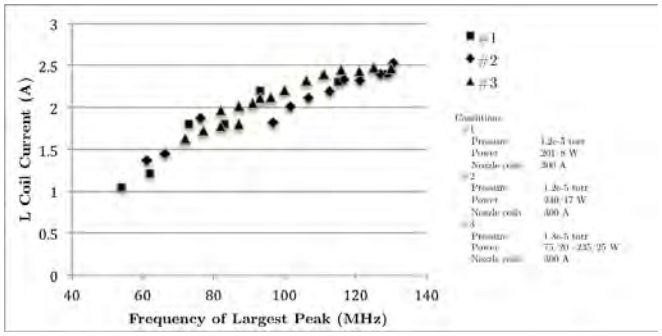

FIG. 3. Plotting low-range frequency peaks vs. L-coil current shows a linear relationship.

It was found that these low frequency modes interacted with the dominant 27 MHz signal to produce side bands around the main signal, spaced corresponding to the peak structure found around 1-2 MHz. The amplitudes of these side bands, however, did not match up as closely.

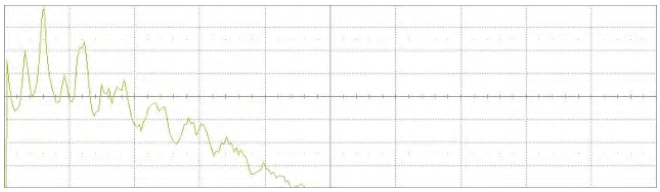

(a) 62 A

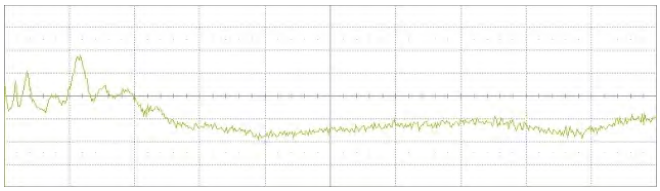

(b) 115 A

FIG. 4. Examples of low-frequency peak structure at different L-coil currents.

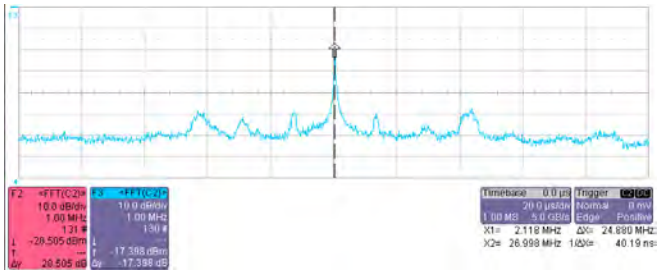

FIG. 5. Example of asymmetrical sideband.

The radial position of the Langmuir probe was adjusted in increments of 0.56 cm to investigate the rotational aspects of the modes we were observing at 1-2 MHz and 27 MHz. The results, taken from three separate trials, were not very consistent, although some general trends were evident. The amplitude of the peaks around 2 MHz decreased as the probe's distance from the center of the plasma column increased, as expected. We once found an anomalous spike in amplitude at 1.27 cm, but the other set of pertinent data points were sufficient to neither confirm nor deny this spike. It is very unlikely that it is related to coils interfering with the field lines, as shown in Fig. 7. The diagram clearly shows that at z = 80 cm, where the probe is located, the field lines that do not intersect a solid surface extend to 3 cm from the center. Because conditions change there, we would expect to see abnormal behavior at r = 3 rather than at r = 1.27. The data pertaining to the 27 MHz signal was also inconsistent; in one case, the amplitude of the signal stays almost constant, while the other trial shows a clear decrease, excepting another anomalous point at r = 0.31 cm. Since all of these modes are observed at the center of the column, none of these modes are m = 1 or greater.

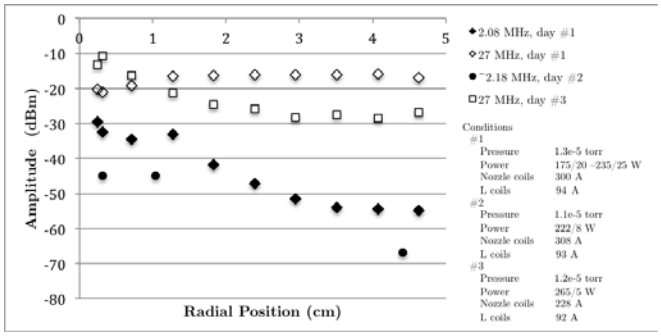

FIG. 6. Amplitude of input and low frequency peaks vs. radial position of Langmuir probe.

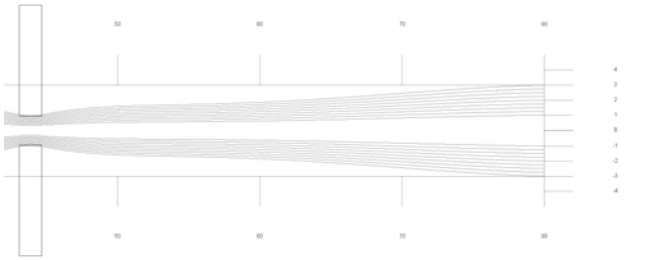

FIG. 7. Magnetic field lines around the probe, located 80 cm from the center of the machine along the z-axis.

Connecting the Langmuir probe to an oscilloscope whose probe had higher impedance, we found that the original oscilloscope had not been showing the true floating potential because the probe within the oscilloscope was letting current through. With the higher impedance, we could measure the actual potential, which had a DC offset of over -250 V. As the RF power increases, all other factors constant, the plasma heats up and the average floating potential decreases. The data meets this expectation, with the exception of the point at 120W, which is lower than anticipated compared to the other data points.

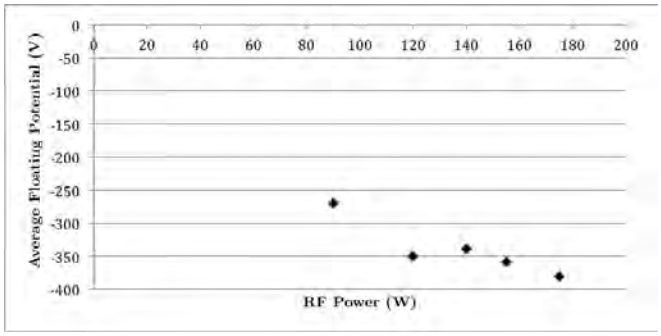

FIG. 8. Average floating potential plotted against RF power shows a near-linear relationship.

On the highest end of the spectrum, we consistently found a broad peak around 300 MHz, which is in the

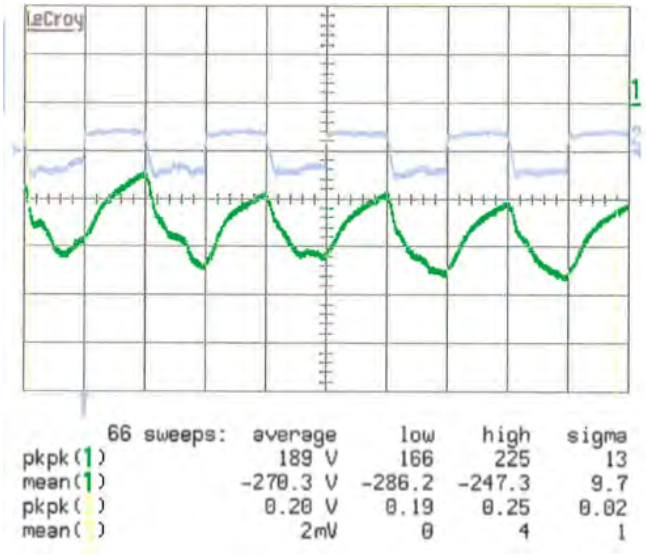

(a) 90 W

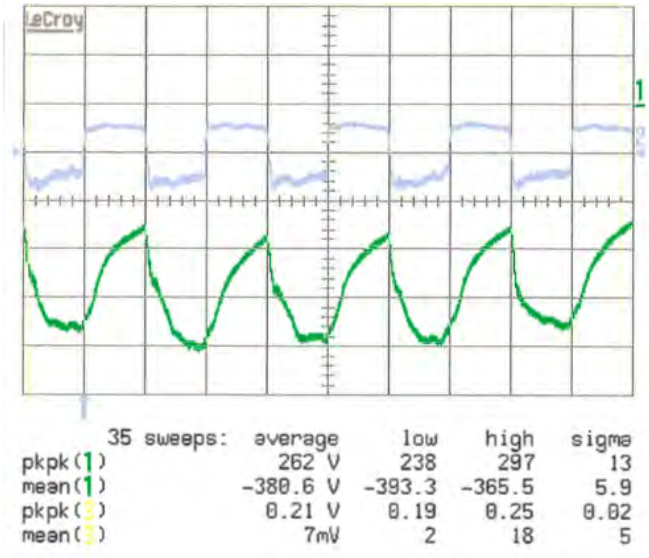

(b) 175 W

FIG. 9. Example screenshots at different power levels. Power is modulating at 5 kHz.

range of the electron cyclotron frequency and electron plasma frequency.

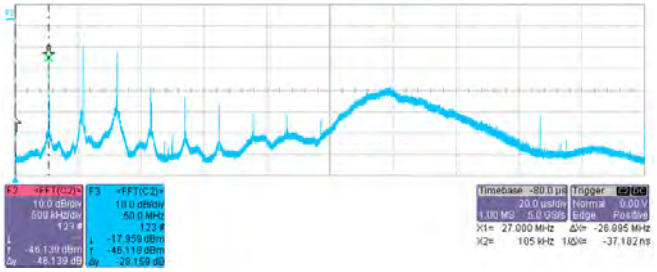

FIG. 10. Example of the broad peak near 300 MHz.

On two separate occasions we found very low frequency bursting modes in the plasma. They are suspected to be different because of the small but non-negligible difference in frequency. Each was only found once. Fig. 11(a) shows oscillations from the Langmuir probe (in pink) and from a pickup coil taped to the outside of the PFRC (in blue). We do not have Fourier transforms of these oscillations to confirm or rebut these bursts, which have a period of 360 Hz. This mode was not seen again. Fig. 11(b) show measurements from the probe, on a different day. The conditions are different, but the second measurements were made with a low-pass filter with a limit of 1.9 MHz to better examine the 100 Hz range. This spectrum shows a well-defined peak at 400 Hz. The turbo pumps, which also operate at 400 Hz, may be the cause, but this has not been confirmed.

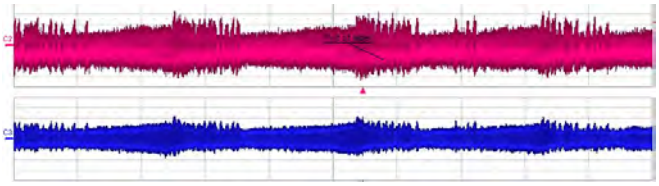

(a) 1.00 ms/div

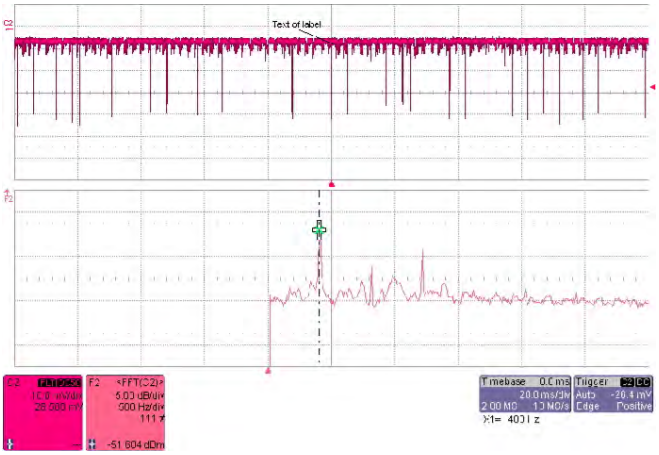

(b) Time scale and Fourier transform.

FIG. 11. Very low frequency bursting modes.

Without the RMF, the plasma was dim enough that fast camera videos could only be taken when argon was present in the PFRC. The limited frame speed also limited the frequency of observable oscillations. Videos 1 & 2 were shot at the same conditions:

L coils	92 A
Nozzle coils	300 A
P_{in}/P_{out}	228/15
Pressure (H)	4.85e-5 torr
Pressure (Ar)	2.66e-6 torr

The video in link 1 was shot at 5 kfps with an exposure time of 190μs, playing at 10fps. A smooth, pulsing oscillation is visible, with frequency 527 ± 40 Hz. In the second video, however, the plasma's motion looks very different despite no change having been made. Here, it appears that the column is rotating around the z-axis, although the motion appears much more erratic. The oscillation in this video is 676 ± 20 Hz.

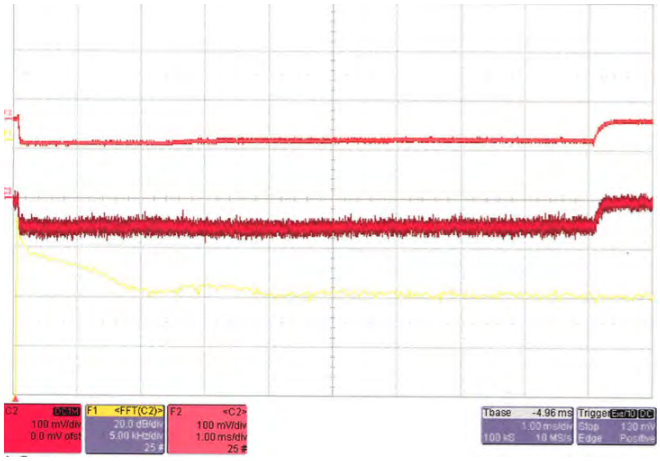

FIG. 12. Density fluctuation was measured with an interferometer. Density increases when the RMF turns on (the red traces are inverted), and decays 9 ms after. The noisier red trace shows the measured potential; the smoother red line is the first traced, averaged.

With the FRC, the plasma emitted enough light to allow videos at much higher frame speeds. Density fluctuations (Fig. 12) closely matched the growing oscillations visible in video 3. With the introduction of the hydrogen puff in the same video, the plasma appears to settle, with no more apparent fluctuations. The brightest part of the plasma moves toward the center of the machine while the plasma closer to the nozzle coils dims. Occasionally, the power from the RMF does not properly couple to the plasma, and we measure much higher reflected back. Video 5 shows an example of this phenomenon.

Video Links

Plasma column

1. https://goo.gl/ewVJEH
2. https://goo.gl/mb1IPV

FRC

3. https://goo.gl/LXEW1W
4. https://goo.gl/JcEiIE
5. https://goo.gl/nNd6NA

IV. DISCUSSION

In trying to understand the frequencies in the 1-2 MHz range, we theorized that some of the fundamental plasma oscillations may be causing the frequencies we found: ion or electron cyclotron frequencies, or ion or electron plasma frequencies. The values for these frequencies are given as follows:

$$f_{ci} = 1.52 \times 10^3 Z\mu^{-1} B \text{ Hz} \quad (1)$$

$$f_{ce} = 2.80 \times 10^6 B \text{ Hz} \quad (2)$$

$$f_{pi} = 2.10 \times 10^2 Z\mu^{\frac{-1}{2}} n_i^{\frac{1}{2}} \text{ Hz} \quad (3)$$

$$f_{pe} = 8.98 \times 10^3 n_e^{\frac{1}{2}} \text{ Hz} \quad (4)$$

where $Z = +1$ is the ion charge, B is the magnetic field strength, n_i and n_e are the ion and electron number densities, respectively, and $\mu = 2$ is the ion-to-proton mass ratio. Because we ran with only hydrogen in the PFRC, we know $n_i = n_e$. Using measurements of number density from the main chamber, we can estimate and place an upper bound on n in the satellite region around $3.0 \times 10^8 - 3.5 \times 10^10$. The oscillations could originate from anywhere within the plasma column, so from Fig. 2, we know $\vec{B}$ is between 50 and 2800 G. For a non-specific $\vec{B}$ in this range, we have:

$f_{ci} : 38,000 - 2,100,000$ Hz
$f_{ce} : 140,000,000 - 7,800,000,000$ Hz
$f_{pi} : 2,600,000 - 27,000,000$ Hz
$f_{pe} : 160,000,000 - 1,700,000,000$ Hz

Both the ion cyclotron frequency and the ion plasma frequency are in the correct range. From the near-linear movement of the peaks in the $\vec{B}$ scan, we believe that these are related to the ion gyrofrequency. It could also be the electrostatic ion cyclotron wave, which shares the same frequency.

There is often a degree of asymmetry in the side bands surrounding the 27 MHz peak. This we associate with a parametric instability, which is an interaction between two waves, in this case the 1-2MHz and the RF signal, that results in a third wave whose frequency is spaced from the larger of the first two waves by the frequency of the smaller. This describes what we see in Fig. 5, except for the fact that parametric instabilities normally appear in the Fourier transform on the lower frequency (left) side of the peak, and we found asymmetrical side bands just as often on the other side. While this type of instability often appears only above a certain power threshold[1], we were unable to test this because the power of the RF signal could only be lowered to a certain level while still sustaining the plasma.

The large DC offset that appears when using the other oscilloscope indicates a population of hotter electrons. Before finding this large negative potential, the only suggestion of such high temperatures within the plasma was X-ray emission, which was completely unexpected prior 'to this new oscilloscope data. What we have found agrees with the X-ray data in an accompanying paper to be published in APS by Jandovitz, et al. The negative offset is due to a negatively charged sheath forming around the surface of the probe because the electrons move much faster than ions as a result of their

[1] M. Porkolab and R. P. H. Chang, Rev. Mod. Phys. 50, 745 (1978).

smaller mass. The probe becomes more and more negatively charged until the sheath attracts protons and repels electrons enough to counteract the faster-moving electrons bombarding the probe. Before, with the first oscilloscope, the impedance was too low and allowed current to flow, but with the other oscilloscope, we were able to more accurately measure the floating potential. By increasing the RF power, the plasma temperature, as well as electron temperature, increases. This means that the probe's sheath must be more negatively charged to reach equilibrium between proton attraction, electron repulsion, and fast-moving electrons. The offset is approximately linearly related to the power sent into the plasma, as we would expect from Eq. 5[2].

$$\frac{eV_f}{T_e} = \frac{1}{2}[\ln(2\pi\frac{m_e}{m_i}) - 1] \tag{5}$$

With $e = 1$ V_f 300, we have T_e 80 eV. However, this represents the average temperature between the larger, cooler electron population and the hotter population that is emitting electrons. Because we can only calculate the average, we cannot find the temperature of the hot population; however, Jandovitz, et al. measured temperatures as high as 2 keV.

From the Phantom videos, we can see instabilities growing with time, as well as the stabilizing effect of the hydrogen gas puff. We can also roughly estimate the time it takes for the plasma to reach full brightness when the RMF turns on and to return to its 'regular' brightness. Video 4, shot at 121,212 fps with an exposure of 3 μs, shows that 3 frames pass, so the actual rise time is between 16.5 and 24.8 μs. The fall takes 2 frames, so fall time is between 8.25 and 16.5 μs.

V. CONCLUSION

Studying and understanding the oscillations in plasma are fundamental to learning how plasma behaves. Oscillations are essential in general for their relation to instabilities, but they are particularly important for the PFRC because it is radio frequency waves that produce the plasma. In this paper, we examined oscillations at frequencies as low as 400 Hz to about 300 MHz. We found that in the 1-2 MHz range, frequencies vary linearly with magnetic field strength, pointing to the ion gyrofrequency as the cause. These waves interacted with our injected signal and produced complex sideband structures. Most unexpectedly, we found that the probe actually carries a large negative potential, which corroborates X-ray data suggesting the existence of a population of higher temperature electrons.

VI. ACKNOWLEDGEMENTS

I would like to thank Dr. Cohen for the giving me the opportunity to participate in the PFRC group, to learn about experimental plasma physics, and to experience work as a researcher. I also want to thank Charles Swanson for all the time he spent helping me throughout the summer, from explaining various concepts to setting up the Phantom camera.

I owe much to the Princeton Environmental Institute for funding this internship. The PFRC is supported by DOE contract DE-AC02-09CH11466.

[2] I. H. Hutchinson. *Principles of Plasma Diagnostics,* 2nd Ed. (Cambridge University Press, Cambridge, 2005), p. 71.